Broadband ultraviolet light source using GaN quantum dots formed on hexagonal truncated pyramid structures

Jong-Hoi Cho[a,†], Seung-Hyuk Lim[a,d,†], Min-Ho Jang[a], Chulwon Lee[a], Hwan-Seop Yeo[a], Young Chul Sim[a], Je-Hyung Kim[a], Samuel Matta[b], Blandine Alloing[b], Mathieu Leroux[b], Seoung-Hwan Park[c], Julien Brault[b], and Yong-Hoon Cho[a,*]

[†]: Equally contributed

[1] Department of Physics and KI for the NanoCentury, Korea Advanced Institute of Science and Technology (KAIST), Daejeon 34141, Republic of Korea

[2] Université Côte d'Azur, CNRS, CRHEA, 06560 Valbonne, France

[3] Department of Electronics Engineering, Catholic University of Daegu, Kyeongsan 38430, Republic of Korea

Correspondence: Yong-Hoon Cho (email: yhc@kaist.ac.kr).

[4] Present address: R&D Investment planning team, Korea Institute of S&T Evaluation and Planning (KISTEP), Seoul 06775, Republic of Korea

Statistics of the shape and density of B- and P-QDs

Using the SEM images, we investigated morphological shape as well as density of B- and P-QDs, respectively. As shown in Figure S1, Maganified SEM image of truncated pyramid sturcture at the center and edge were measured, respectively. The P-QDs were densly formed on the surface. On the otherhands, the B-QDs were not only sparsely formed, but also distributed along the boundary line as representing in Figure S1 (c) (yello dashed-line). Consequently, a dentisy of B-QDs was estimated to be $4.80 \pm 0.31 \times 10^{10} cm^{-2,}$, which was smaller than that of P-QDs ($5.88 \pm 0.82 \times 10^{10} cm^{-2}$).

Furthermore, we found that the morphological shape of B-QDs was closed to the epiilsoidal shape rather than circular shape. Especially, the elongated direction was $[0\bar{1}0]$ corresponding to the stretched lattice at the boundary region. The ratios between major- and minor-axis of B- and P-QDs were investigated, where they were 2.37 ± 1.19 and 1.29 ± 0.47, respectively.

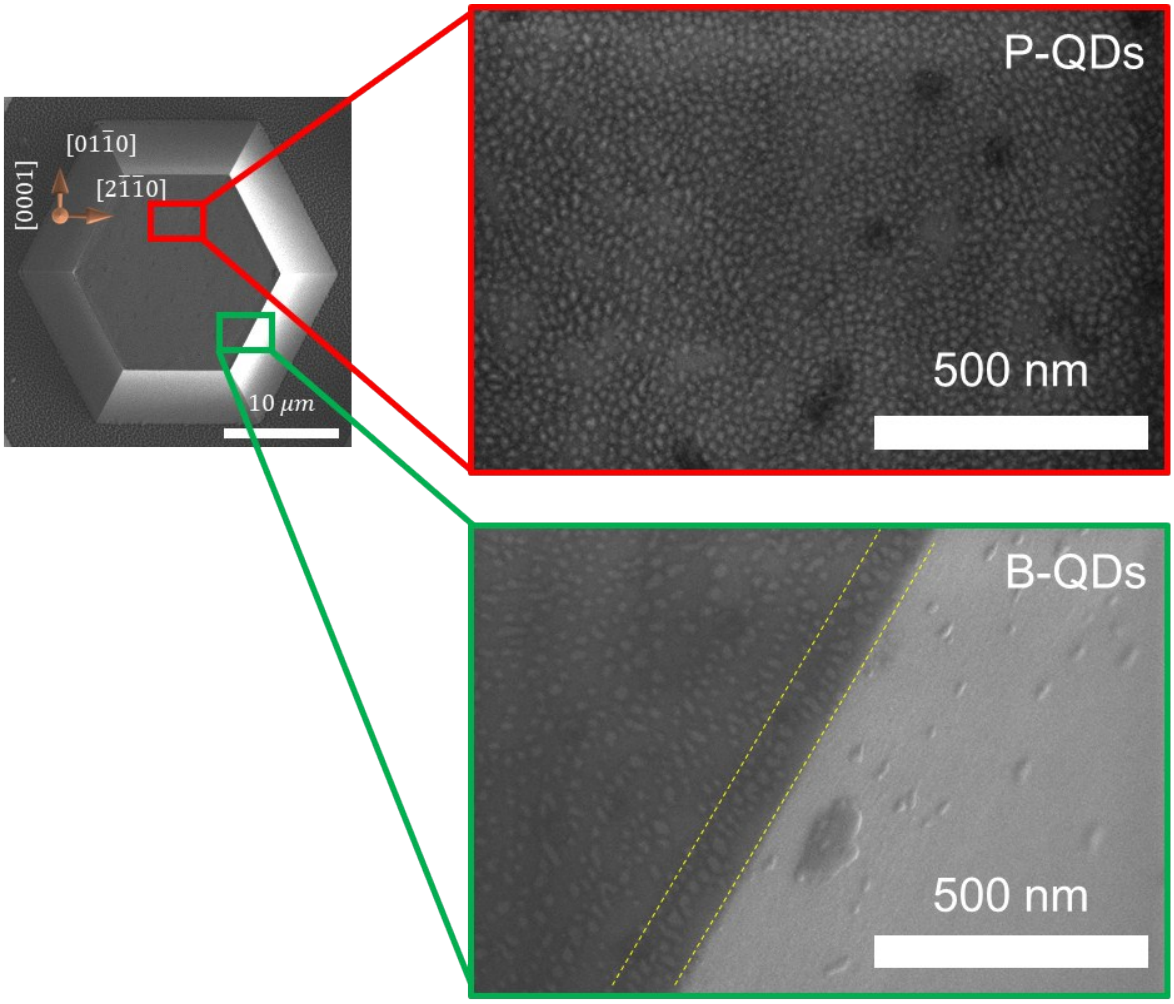

	B-QDs	P-QDs
Density (10^{10}cm^{-2})	4.80±0.31	5.88±0.82

Figure S1. SEM image of GaN QDs embedded in trucated pyramid structure. (a) Top-view image of whole truncated pyramid structure. (b)-(c) Magnified top-view image of truncated pyramid structure at center and edge, repetively, where yellow dahsed-line indicates B-QDs. (d) Density of B- and P-QDs, repectively.

Computational strain analysis of the AlxGa1-xN layer below the B- and P-QDs

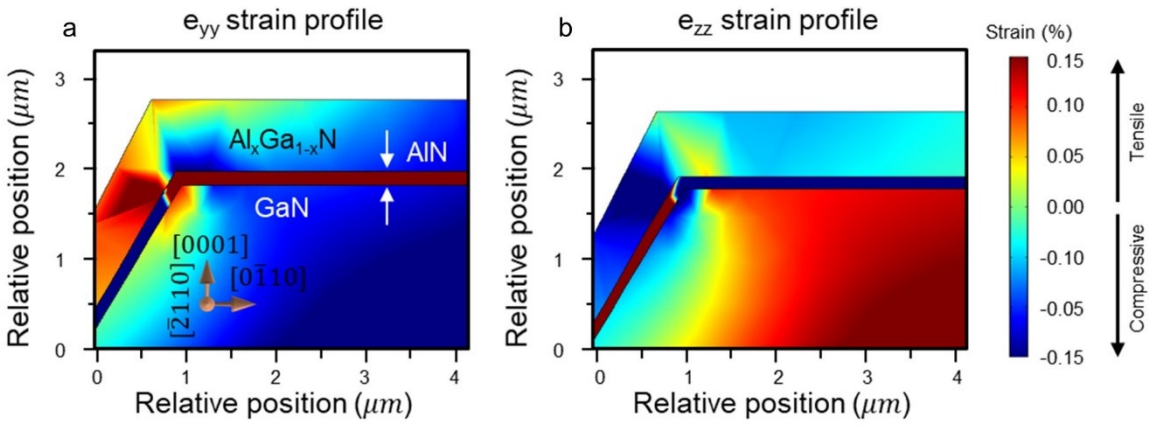

Figure S2 Computational strain profiles of (a) e_{yy} and (b) e_{zz} near the boundary region of the truncated pyramid structure.

Using calculations, we investigated the strain profile of e_{yy} and e_{zz} as shown in Figure S2(a) and S2(b), respectively. Compared to the initial parameters of the $Al_xGa_{1-x}N$ lattice, the $Al_xGa_{1-x}N$ lattice at the boundary region was stretched less than 0.05% along the direction {10$\bar{1}$0}, while it had shrunk less than -0.03% along the direction (0001). Although the stretched value of $Al_xGa_{1-x}N$ lattice parameters from the SAD pattern (Figure 4b and 4c in the manuscript) and calculations are not identical, it is quite clear that the boundary region of the truncated pyramid structure can relax the strain. Consequently, the stretched lattice at the boundary region reduced the lattice mismatch with GaN QDs.

CL spectra using local exciation

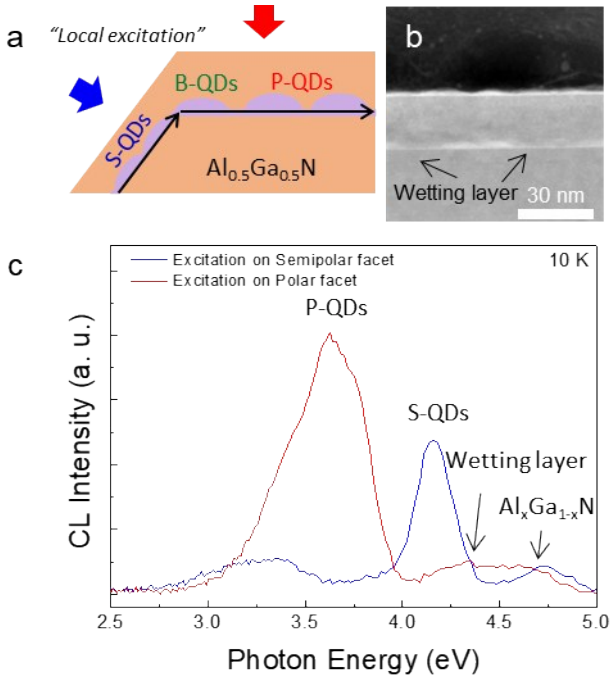

Figure S3. (a) Schematic of local excitation on polar and semipolar facets. (b) HRTEM side-view images, where arrow indicates a GaN wetting layer (c) CL spectra of polar (red solid line) and semipolar (blue solid line) facet via local exciation.

Figure S3 shows that the CL spectra through the local excitation on the polar and semipolar facets, respectively. Although there were the GaN wetting layer as well as QDs and $Al_xGa_{1-x}N$ layer, the emission wavelength of GaN wetting layer was not clearly distinguished due to their broad spectrum. To clarify the emission wavelength of GaN wetting layer, we performed the local exciation on the polar and semipolar facets, respectively. When locally excitation on the polar facet (red solid line in Figure S3(c), we clearly observed not only the emission of B- and P-QDs, but also the

emission of GaN wetting layer and $Al_xGa_{1-x}N$ layer, which was well congruent with previous our works.[1-3] For local excitation on the semipolar facet, the emission of $Al_xGa_{1-x}N$ layer was obviously observed, but the emission of GaN wetting layer was overlapped with S-QDs due to not different emission wasvelength between GaN wetting layer and S-QDs. It indicates small band off-set energy between GaN wetting layer and S-QDs, which leads to weak carrier localization in S-QDs with rising temperatrue.

References

1. Brault J*, et al.* Tailoring the shape of GaN/Al[sub x]Ga[sub 1−x]N nanostructures to extend their luminescence in the visible range. *J Appl Phys* **105**, 033519 (2009).

2. Matta S*, et al.* Influence of the heterostructure design on the optical properties of GaN and Al0.1Ga0.9N quantum dots for ultraviolet emission. *J Appl Phys* **122**, 085706 (2017).

3. Leroux M*, et al.* Stark effect in ensembles of polar (0001) Al0.5Ga0.5N/GaN quantum dots and comparison with semipolar (11−22) ones. *J Appl Phys* **116**, 034308 (2014).